



<b>Publication Year</b>	2020
<b>Acceptance in OA</b>	2023-02-09T13:52:55Z
<b>Title</b>	VTX-TN12_Technical_Budgets
<b>Authors</b>	MORETTI, Alberto, Tordi, M., Zocchi, F., USLENGHI, MICHELA, Amisano, F.
<b>Handle</b>	<a href="http://hdl.handle.net/20.500.12386/33336">http://hdl.handle.net/20.500.12386/33336</a>

# VERT-X Design of Vertical X-Ray Test Facility for ATHENA

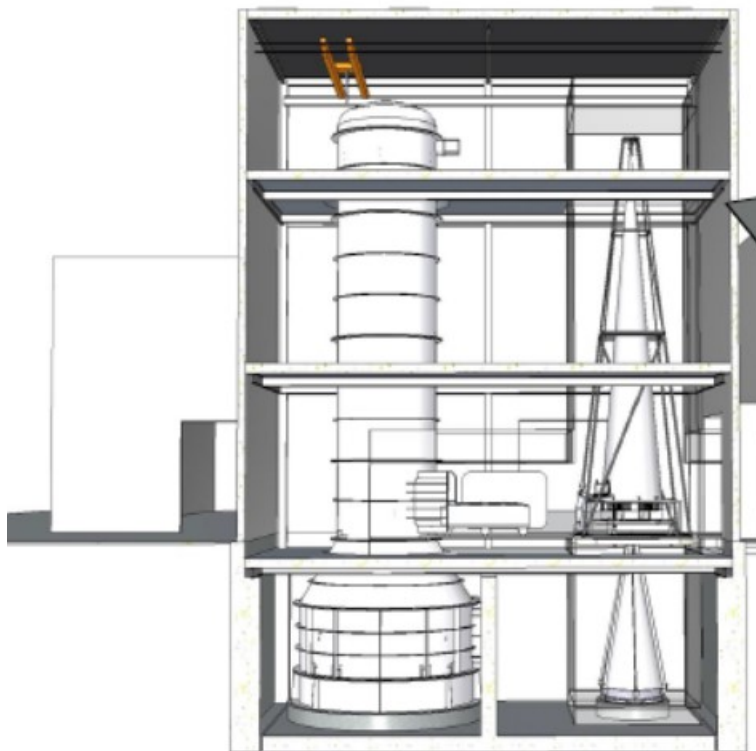


## VERT-X Design of Vertical X-Ray Test Facility for ATHENA

### TN12 TECHNICAL BUDGETS

Doc: VTX-OAB-ISE-TEC-001

Date: 17 / 04 / 2020



## VERT-X Design of Vertical X-Ray Test Facility for ATHENA



### CHANGE RECORDS

ISSUE	DATE	AUTHOR	APPROVED	QA/QC	SECTION / PARAGRAPH AFFECTED	REASON/INITIATION Documents/Remarks
I01p00	23/10/2019				All	First Issue
I01p01	20/12/2019				3 and 4	Inserted error budgets
I01p02	17/04/2020				3.1 and 3.3	Inserted effective area error budget

### AUTHORS AND RESPONSIBLES

Document:	VTX-OAB-ISE-TEC-001		
Issue:	I01p01		
Date:	17/04/2020		
Prepared by:	A. Moretti (INAF – OAB)	Signed by :	
	M. Tordi (EIE)		
	F. Zocchi (MLS)		
	M. Uslenghi (INAF – IASF)		
	F. Amisano (GPAP)		
Checked by:	Alberto Moretti (INAF - OAB)	Signed by:	
Approved by:	Stefano Basso (INAF - OAB)	Signed by:	
Released by:	Alberto Moretti (INAF - OAB)	Signed by:	

### CONTRIBUTING ENTITIES

INAF – OAB	Partner
INAF - IASF	Partner
Media Lario	Partner
EIE	Partner
GP Advanced Projects	Partner
BCV	External Service

# VERT-X Design of Vertical X-Ray Test Facility for ATHENA



---

## TABLE OF CONTENTS

1. INTRODUCTION.....	4
1.1. SCOPE .....	4
1.2. APPLICABILITY .....	4
1.3. ROADMAP .....	4
2. APPLICABLE AND REFERENCE DOCUMENTS .....	5
2.1. APPLICABLE DOCUMENTS.....	5
2.2. REFERENCE DOCUMENTS.....	5
2.3. GENERAL SPECIFICATIONS AND STANDARD DOCUMENTS .....	5
2.4. LIST OF ACRONYMS.....	6
3. MEASURE ERROR BUDGETS .....	7
3.1. HEW Error budget.....	7
3.2. A more general approach .....	9
3.3. Effective area error budget .....	10
4. TECHNICAL BUDGETS.....	13
4.1. MASS BUDGET .....	13
4.2. POWER BUDGET .....	14
5. VERT-X ELEMENTS BUDGET DETAILS.....	15
5.1. THERMAL VACUUM CHAMBER .....	15
5.2. XRS TESTING SYSTEM .....	22
5.3. X-RAY SOURCE AND COLLIMATOR.....	23
5.4. DETECTION ASSEMBLY .....	24

## 1. INTRODUCTION

### 1.1. SCOPE

The scope of the present document is the illustration of VERT-X technical budgets, according to the outcomes of the System Requirements Review (SRR), the updates of SOW requirements after the SRR and the design suggestions provided by ESA.

### 1.2. APPLICABILITY

The present document is one of the Preliminary Design Review (PDR) deliverables. It is intended to provide a summary of technical data derived from VERT-X preliminary design activities as well as a reference for the technical budgets definition in the next phases of the study.

Details of technical budgets for the VERT-X facility elements are expected to be updated and expanded with the evolution of VERT-X design.

### 1.3. ROADMAP

Document section	Content description
Section 2 (Applicable and reference documents)	List of applicable documents and reference documents.
Section <b>Error! Reference source not found.</b> (System level budgets)	Presentation of VERT-X facility preliminary technical budgets at system level.
Section 5 (VERT-X elements budgets details)	Technical budget details for the main VERT-X facility elements.

Table 1-1: Roadmap of the document

# VERT-X Design of Vertical X-Ray Test Facility for ATHENA



## 2. APPLICABLE AND REFERENCE DOCUMENTS

### 2.1. APPLICABLE DOCUMENTS

AD1	AO/1-9549/18/NL/AR - SOW	X-ray Raster Scan Facility for the ATHENA Mirror Assembly SOW
AD2	VERT-INAFOAB-001	VERTICAL X-Ray (VERT-X) Technical Proposal
AD3	ESA-TECMMO-RS-014713	Updated Requirements for the ATHENA VERT-X following the System Requirements Review

### 2.2. REFERENCE DOCUMENTS

RD1	VTX-OAB-ISE-REP-001 - Conceptual Design Report
RD2	VTX-OAB-ISE-REP-002 - Trade-off Report
RD3	ATHENA - MCF URD, IRD & ICD ISSUE 1.3 [ESA].pdf
RD4	ATHENA - Calibration Requirements Document, ESA-ATH-SP-2016-001, issue 0.5.1.pdf
RD5	ATHENA - Optics Calibration Plan, ESA-ATHENA-ESTEC-SCI-PL-0001, Issue 1.1.pdf
RD6	ATHENA - Acronyms and Definitions ATHENA-ESA-LI-0001
RD7	VTX-EIE-ISE-TEC-002 Raster Scan System
RD8	VTX-MLT-ISE-TEC-001 X-ray Source and Collimator System
RD9	VTX-OAB-ISE-TEC_TN11 Concept of Operation
RD10	STRAY-LIGHT simulation, rw_stray_xrays_Feb_2019, Willingale R. 2019

### 2.3. GENERAL SPECIFICATIONS AND STANDARD DOCUMENTS

SD1	ECSS-M-40A	Configuration management
SD2	ECSS-M-50A	Information/documentation management

## VERT-X Design of Vertical X-Ray Test Facility for ATHENA



### 2.4. LIST OF ACRONYMS

AD	Applicable Document
EA	Effective area
EIE	EIE Space Technologies
ESA	European Space Agency
GPAP	GP Advanced Projects
I/F	Interface
IASF	Istituto di AstroFisica Spaziale (INAF, Milano)
INAF	Istituto Nazionale di AstroFisica
ITT	Invitation To Tender
MA	Mirror Assembly
MLS	Media Lario S.r.l.
OAB	Osservatorio Astronomico di Brera (INAF, Milano)
PDR	Preliminary Design Review
RD	Reference Document
SD	Standard Document
SOW	Statement of Work
SRR	System Requirements Review
TBA	To Be Assessed
TBC	To Be Controlled
TBD	To Be Defined
TEC	Technical Note
TVC	Thermal Vacuum Chamber
VERT-X	VERTICAL X-Ray
VTX	VERT-X
XRS	X-ray Raster Scanner
XYZS	(x, y, z) Stage

## 3. MEASURE ERROR BUDGETS

Requirements on the PSF are present both in the AD3 and RD4 with some differences. In AD3, the required uncertainty of the HEW both for the verification and calibration phases is 1" for all energies, on- and off-axis angles, with a goal of 0.5" at 99.73% confidence. On the other the RD4 requires an error of 0.1" at 68% confidence together with a 5% uncertainty on the EEF of the wings and the halo.

### 3.1. HEW Error budget

The most direct way of measuring the HEW of an X-ray telescope ( $HEW_{MA}$ ) and its PSF is, by construction, the observation of a point-like celestial source when the telescope is in flight. In this case the measure is free of significant systematics, with the statistical error as the main uncertainty source. Minor systematic uncertainties can be given by the detector pixel size, the wobbling of the satellite and the event reconstruction.

On the other hand, the HEW measured during on-ground calibration, as in the case of VERT-X, will be affected by several systematic errors. In fact, the on-ground measure of the HEW of ATHENA MA ( $HEW_{VTX}$ ) will be the result of the (quadratic) sum of  $HEW_{MA}$  with several independent contributions.

We individuate the pointing uncertainty ( $HEW_{PNT}$ ), the source dimension ( $HEW_{SOU}$ ), the mirror error ( $HEW_{MIR}$ ), the relative position between source and collimator ( $HEW_{FOC}$ ) and the gravity induced distortions ( $HEW_{GRV}$ ) as the major ones. The HEW that we will measure at VERT-X will be given by:

$$HEW_{VTX}^2 = HEW_{MA}^2 + HEW_{PNT}^2 + HEW_{SOU}^2 + HEW_{MIR}^2 + HEW_{FOC}^2 + HEW_{GRV}^2,$$

where  $HEW_{MA}$  is the quantity we aim at calibrating and  $HEW_{VTX}$  is what we measure.

As shown in RD8 the two quantities  $HEW_{MIR}$  and  $HEW_{SOU}$  combine together linearly. Therefore hereafter we consider them as one single term, named  $HEW_{SYS}$

$$HEW_{VTX}^2 = HEW_{MA}^2 + HEW_{PNT}^2 + HEW_{SYS}^2 + HEW_{FOC}^2 + HEW_{GRV}^2,$$

Inverting the equation we have that

$$HEW_{MA}^2 = HEW_{VTX}^2 - HEW_{PNT}^2 - HEW_{SYS}^2 - HEW_{FOC}^2 - HEW_{GRV}^2, \quad (3.1.1)$$

which is nothing else than a de-convolution. While the measure of  $HEW_{MA}$  is the goal of the calibration, at the VERT-X facility we will measure  $HEW_{VTX}$ .  $HEW_{MA}$  measure will be obtained by de-convolving the known error terms. The calibration requirement on the HEW AKE ( $HEW < 0.1''$ , RD4) has to be compared with the error on this de-convolution  $\sigma_{HEW\_MA}^2$ .

To calculate the expected value for the  $\sigma_{HEW\_MA}^2$ , first, for simplicity, let's assume that B is the convolution of only two terms

$$B^2 = A^2 + C^2, \text{ where } A \text{ is the quantity we want to measure.}$$

A will be given by the deconvolution:

$$A^2 = B^2 - C^2, \text{ i.e. } A = \sqrt{B^2 - C^2}.$$

The error on A, that we call  $\sigma_A$  can be calculated by the error propagation formula

$$\sigma_A = \sqrt{\left(\frac{\partial A}{\partial B}\right)^2 \sigma_B^2 + \left(\frac{\partial A}{\partial C}\right)^2 \sigma_C^2} ;$$

since  $\frac{\partial A}{\partial B} = \frac{1}{2} 2B (B^2 - C^2)^{-\frac{1}{2}} = \frac{B}{A}$ , it comes that

$$\sigma_A = \sqrt{\left(\frac{B}{A}\right)^2 \sigma_B^2 + \left(\frac{C}{A}\right)^2 \sigma_C^2} .$$

The error on the deconvolution is given by the quadratic sum of the error on the original term B with the error on the deconvolved term C, with both terms weighted by the (quadratic) ratio with A.

In the same way, for  $\sigma_{HEW\_MA}^2$ , we obtain

$$\sigma_{HEW\_MA}^2 = \frac{HEW_{VTX}^2}{HEW_{MA}^2} \sigma_{HEW\_VTX}^2 + \frac{HEW_{PNT}^2}{HEW_{MA}^2} \sigma_{HEW\_PNT}^2 + \left(\frac{HEW_{SYS}^2}{HEW_{MA}^2}\right) \sigma_{HEW\_SYS}^2 + \frac{HEW_{MIR}^2}{HEW_{MA}^2} \sigma_{HEW\_FOC}^2 + \frac{HEW_{GRV}^2}{HEW_{MA}^2} \sigma_{HEW\_GRV}^2 .$$

The uncertainty on the  $HEW_{MA}$  will be given by the (quadratic) sum of the uncertainties of each single term, weighted by the ratio with the intrinsic  $HEW_{MA}$ . The amplitudes of different contributions to the total error budget are discussed in separate documents and are here reported in Table 2.

As it is clear from the table, since all the systematic contributions are kept at the level  $\cong 1''$  or less, their weights in the error budget are minor, with the main term being the statistical error.

Indeed, the statistical term is the only one with a weight of the order of the unity. As discussed in RD9,

for each energy bin, we plan to collect 50,000 photons from the calibration source corresponding to an expected statistical uncertainty of 0.05".

We stress that keeping the systematics at a level of few percent of the  $HEW_{MA}$  is doubly valuable.

First, as already said, in the error budget each term is weighted by its ratio with the HEW itself.

Second, each term is a factor in  $HEW_{VTX}$ , directly affecting the weight of the statistical error. In other words, if the systematic terms ( $HEW_{PNT}$ ,  $HEW_{SOU}$ ,  $HEW_{MIR}$ ,  $HEW_{GRV}$ ) were comparable to  $HEW_{MA}$ , the measured  $HEW_{VTX}$  would be  $\gg HEW_{MA}$ , meaning that the weight of the statistical error would be  $\gg 1.0$ .

*Table 2 Preliminary estimate of different contributions to the HEW error budget*

ERROR SOURCE	HEW["]	$\sigma_{HEW}$ ["]	REFERENCE
POINTING	0.27	0.24	RD7
SOURCE	1.00	0.20	RD8
COLLIMATOR	0.55	0.15	RD8
SYS (SOU.+COLL.)	1.55	0.35	RD8
SOU-COLL displ.	0.1	0.1	RD8
GRAVITY	0.1	0.05	RD1
VERT-X MEASURE	5.14	0.05	RD9

(\*) in the case of WOLTER geometry mirror. For a single reflection this value is expected much higher (RD8).

Filling the equation with the numbers here reported, we find that the expected measure HEW, will be 5.14" which allows us to estimate the intrinsic  $HEW_{MA}$  with an error of 0.09" at 68% confidence, compliant with the requirements.

To give an idea of the relative weights of these values, in Figure 1, we plot the HEW measured and the total error with the statistical error of 0.05" as in the present case, with systematics at the values reported in Table 2 and varying them by a multiplying factor.

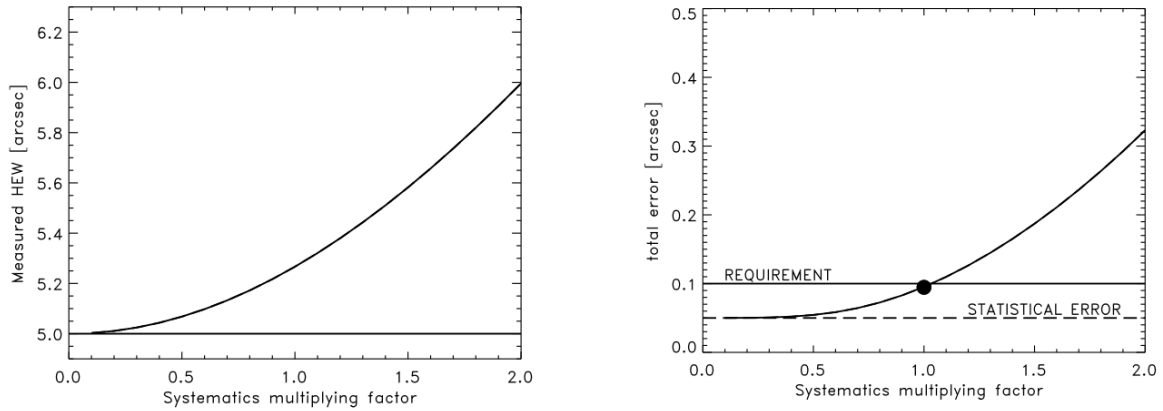


Figure 1 Measured HEW (left) and total error on  $HEW_{MA}$  (right) as function of variations of the systematic contribution. Black point shows the expected error in the current design as described in the text.

The 0.1" requirement on the HEW is motivated by the need of keeping the uncertainty in the flux measure below 1%. It is shown that, with an error of 0.1" on the HEW together with a 5% accuracy on the EEF at larger radii, the photometric error is below 1%. However, this might be interpreted as the requirement on the flight calibration, which, as said, is free from systematic errors. The experience from previous missions showed that the PSF model produced by on-ground calibration data-sets can be easily corrected and improved by means of flight data in the early phases of the missions.

### 3.2. A more general approach

Starting from Eq 3.1.1, we can get the same result following a more general approach, which allows to put in evidence the assumptions made in the previous paragraph. Each term of Eq. 3.1.1 represents a measurable quantity, with an associated statistics (mean value  $Z_i$  and variance  $\sigma_i$ ), and the HEW can be represented in general as:

$$z^2 = \sum_i z_i^2$$

We are interested in calculating the variance associated to such variable, which is defined as:

$$Var[z^2] \equiv E \left[ \left( \sum_i z_i^2 - E \left[ \sum_i z_i^2 \right] \right)^2 \right]$$

Algebraic manipulation leads to:

$$\begin{aligned}
 Var[z^2] &\equiv E\left[\left(\sum_i z_i^2 - E\left[\sum_i z_i^2\right]\right)^2\right] \\
 &= E\left[\left(\sum_i z_i^2\right)^2 + \left(E\left[\sum_i z_i^2\right]\right)^2 - 2\left(\sum_i z_i^2\right)E\left[\sum_i z_i^2\right]\right] \\
 &= E\left[\left(\sum_i z_i^2\right)^2\right] + E\left[\left(E\left[\sum_i z_i^2\right]\right)^2\right] - 2E\left[\sum_i z_i^2 \cdot E\left[\sum_i z_i^2\right]\right] \\
 &= E\left[\left(\sum_i E[z_i^2]\right)^2\right] + E\left[\left(\sum_i z_i^2\right)^2\right] - 2\left(\sum_i E[z_i^2]\right)^2 \\
 &= E\left[\sum_{i,j} E[z_i^2]E[z_j^2]\right] + E\left[\sum_i z_i^2 \sum_j z_j^2\right] - 2\sum_i E[z_i^2]\sum_j E[z_j^2] \\
 &= \sum_{i,j} E[z_i^2]E[z_j^2] + \sum_i E[z_i^4] + 2\sum_{i \neq j} E[z_i^2 z_j^2] - 2\sum_{i,j} E[z_i^2]E[z_j^2] \\
 &= \sum_i E[z_i^4] - \sum_{i,j} E[z_i^2]E[z_j^2]
 \end{aligned}$$

The last step is obtained by supposing that the variables are statistically independent, hence  $E[z_i^2 z_j^2] = 0$ .

If the statistics associated to any single variable is Gaussian, then we have:

$$\begin{aligned}
 E[z_i^2] &= -\sigma_i^2 \exp\left[-\frac{z_i^2}{4\sigma_i^2}\right] D_2\left(-j \frac{z_i}{\sigma_i}\right) \\
 E[z_i^4] &= -\sigma_i^4 \exp\left[-\frac{z_i^2}{4\sigma_i^2}\right] D_4\left(-j \frac{z_i}{\sigma_i}\right)
 \end{aligned}$$

Where  $D_k\left(-j \frac{z_i}{\sigma_i}\right)$  is the parabolic cylinder function of grade k. The calculation of the several error terms are reported in the respective technical note. By considering the same values listed in Table 2 as input data, we obtain that the RMS error associated to the MA HEW measurement is the same calculated in the previous section.

We remark that there might be further quantities which are strictly speaking “unknowns”, i.e. which are not recognized by the present modelling and whose action on the size of the HEW is therefore not considered in the calculation.

### 3.3. Effective area error budget

Requirements on EA calibration accuracy are given both in terms of absolute and relative calibration. The required AKE for the absolute measure of the effective area is 6% at 10 monochromatic energies. The required AKE for the relative measure of the effective area are 2% and 3% for on- and off-axis measure respectively.

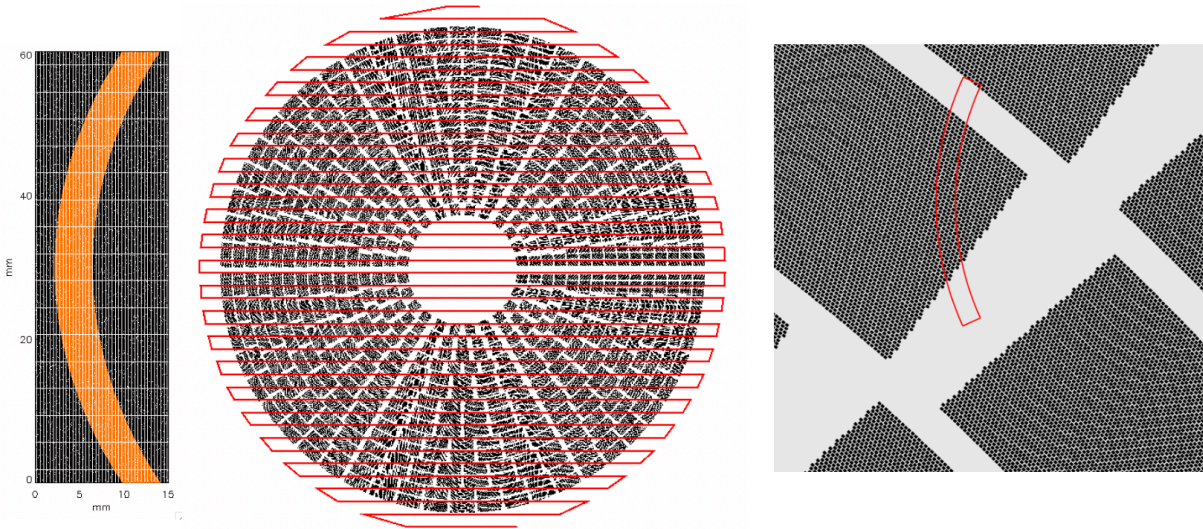


Figure 2 Beam footprint (left) MA (center) masks used to simulate EA calibration test. On the right a zoom of the MA mask, with the beam footprint superimposed is shown

As also described in RD9, the absolute calibration of the MA effective area can be achieved by combining measures of the focused beam, with measures of the beam directly incident on the detector through the central aperture of the MA (hereafter flat-field, FF). In this way the EA measure is straightforward. For each energy E, the effective area measure is given by

$$EA(E) = A_{geo} (C_D(E)/T_D) / (C_F(E)/T_F) F_S F_B$$

where  $C_D$  are the events registered on the detector during  $T_D$  which is the time spent scanning the area  $A_{geo}$  including the MA.  $C_F, T_F$  and  $R_F$  are the values relative to FF measure before, after and during the calibration test.

The above formula assumes that, during the flat-field measure the detector collects a fraction  $F_B$  of the beam. Net variations in the source luminosity are parametrized by the  $F_S$  term. Assuming that the uncertainties in  $T_F$  and  $T_D$  are negligible the EA calibration error budget can be expressed in the following way. Since, by construction, we expect that  $F_B$  and  $F_S$  are very close to the unity, it is evident that the main term in the budget is given by the statistical contribution  $\sigma_{C_D}^2 \sigma_{C_F}^2$  which are discussed in RD9.

$$\frac{\sigma_{EA}^2}{EA^2} = \frac{\sigma_{A_{GEO}}^2}{A_{GEO}^2} + \frac{\sigma_{C_D}^2}{C_D^2} + \frac{\sigma_{C_F}^2}{C_F^2} + \frac{\sigma_{F_S}^2}{F_S^2} + \frac{\sigma_{F_B}^2}{F_B^2} .$$

Inhomogeneity of the MA coverage and border effect are other possible systematic error sources not explicitly covered by the above formula. In order to assess their impact on the final measure we simulated the EA calibration test for a given energy E.

We created a mask reproducing the MA geometry with 0.1mm spatial resolution with 1 at the pore locations and 0 elsewhere. With this resolution pores are described by a 7x5 pixel window (Fig. 2).

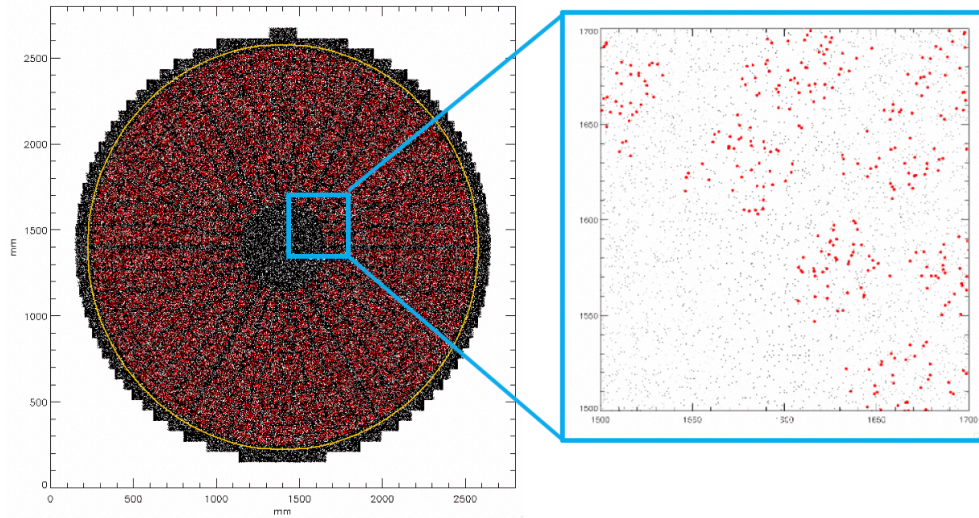


Figure 3 Spatial distribution of all the photons created during a simulation (black dots). Red dots are those which passed through pores and collected by the detector. The yellow circle indicates the area considered for the EA measure, indicated as  $A_{GEO}$  in the formula

Then, we created a mask with the geometry of the beam assuming the footprint described in RD2 and RD9 with the adoption of a mask.

We simulated times and starting positions (within the beam footprint) for a given number of photons. Considering a given energy bin, we assumed a source count rate of 5 ph/s. This produces ~ 2ph/s collected, which is what we expect with 20 energy bins and a suitable count rate of 40 ph/s (RD5 and RD9). Assuming a scan velocity of 5 mm/s this yields ~ 30,000 photons eventually accumulated on the detector.

Given the scan movement and the starting position we assigned a flag to each photon to describe whether it passes through a pore and it is registered by the detector.

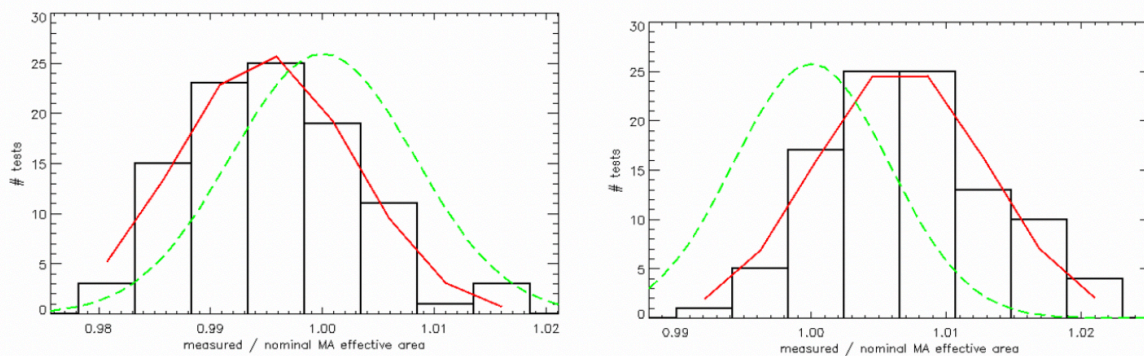


Figure 4 The histogram of the simulation results. Red line is the gaussian fit, green line is the expected value with the only statistical error accounted. Results without and with perturbations included are shown on the left and on the right respectively.

Finally, we considered the times in which the center of the beam was inside within a given circle containing the MA. The size of this circle has been defined in such a way that we can assume that raster scan is moving at nominal velocity with null acceleration.

Following the above formula, we then counted the photons emitted in these good time intervals. As shown in Fig 4 we find a typical systematic difference with the expected value of  $\sim 0.5\%$ . We then perturbed the spatial and time grids with gaussian factors extracted by with 30% sigma distributions. As shown in the right panel of Fig 4, we find that the systematic uncertainties are well below 1%.

Finally, we assessed the impact of inhomogeneity of the scan velocity on the EA measure. Using expected values for the scan velocity variations we find only completely negligible variations. In order to have a significant effect on the measure we should assume variation of at least a factor 10 larger than the expected (RD7).

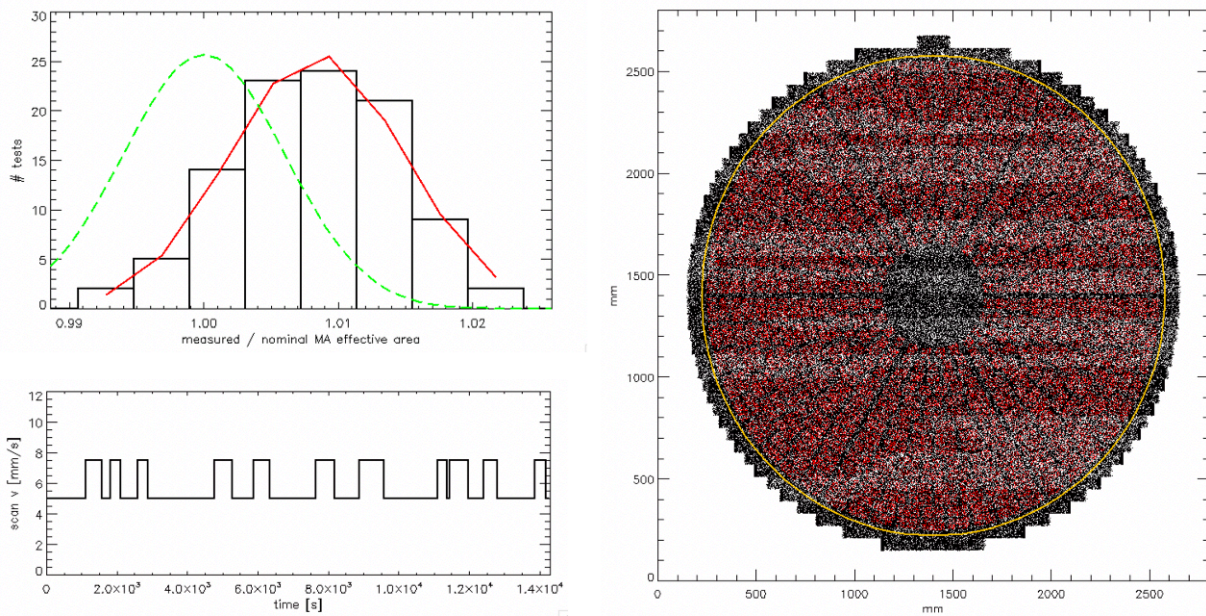


Figure 5 The impact of velocity variation on the EA measure. In the bottom left plot an example of a simulated velocity curve. Velocity variations reflect in inhomogeneity of the MA coverage (right panel); but no significant effect is measured on EA calibration (top left panel).

## 4. TECHNICAL BUDGETS

### 4.1. MASS BUDGET

The mass budget estimation at system level for the current design is listed in Table 4-1.

Preliminary details about mass contributions of the system elements mass, whenever available, are reported in Section 5.

Level 1	Level 2	Description	Mass [kg]
0	0	<b>VERT-X</b>	
3	0	<b>XRS testing system</b>	<b>8340</b>

## VERT-X Design of Vertical X-Ray Test Facility for ATHENA



3	1		raster scan system	7780
3	2		MA system	400
3	3		detection system	TBD
3	4		metrology system	160
4	0	<b>TVC</b>		<b>42113</b>
4	1		vacuum vessel	37783
4	2		vacuum generation system	2930
4	3		cryogenic fluids supp. system	TBD
4	4		thermal control system	1400
6	0	<b>Installation</b>		
6	1		electrical installation	TBD
6	2		system control installation	TBD
<b>Contingency</b>				<b>20%</b>
<b>TOTAL</b>				<b>60544</b>

*Table 4-1: VERT-X general mass budget*

### 4.2. POWER BUDGET

The main contributor to VERT-X power budget is the Thermal Vacuum Chamber (TVC), whose budget details are illustrated in par. 5.1.

The contributions of the X-ray source, collimator and detector assembly may be assumed to be less critical, according to the available design data. Preliminary details about these elements are respectively reported in par. 0 and 5.4, whenever available.

# VERT-X Design of Vertical X-Ray Test Facility for ATHENA



## 5. VERT-X ELEMENTS BUDGET DETAILS

### 5.1. THERMAL VACUUM CHAMBER

Following the preliminary design estimations, mass values of the components of TVC are as reported in Table 5-1. As expected, the vacuum vessel elements are the main contributors.

Part number	Level 1	Level 2	Level 3	Level 4	Level 5	Level 6	Level 7	Mass [kg]
<b>40-00-00-00-00</b>	<b>TVC</b>							<b>39183</b>
<b>41-00-00-00-00</b>		<b>vacuum vessel</b>						<b>37783</b>
41-10-00-00-00			skirt assembly					3673
41-11-00-00-00				welded assembly				3673
41-20-00-00-00			RS segment assembly					11084
41-21-00-00-00				welded assembly				10671
41-22-00-00-00				door assembly				298
41-22-10-00-00				door welded assembly				282
41-30-00-00-00			MA segment assembly					9714
41-31-00-00-00				welded assembly				8929
41-32-00-00-00				door assembly				761
41-32-10-00-00				door welded assembly				761
41-40-00-00-00			detector segment assembly					12049
41-41-00-00-00				welded assembly				11702
41-42-00-00-00				door assembly				298
41-42-10-00-00				door welded assembly				282
41-50-00-00-00			top segment assembly					1263
41-51-00-00-00				welded assembly				1255
<b>42-00-00-00-00</b>		<b>vacuum generation system</b>						<b>2930</b>
42-10-00-00-00			primary vacuum pumps					2604
42-20-00-00-00			turbo-pumps					220
42-30-00-00-00			cryo-pumps					106
<b>43-00-00-00-00</b>		<b>cryogenic fluids supp system</b>						
<b>44-00-00-00-00</b>		<b>thermal control system</b>						<b>1400</b>

Table 5-1: VERT-X TVC mass budget

The following power demand values have been estimated for the vacuum generation system and cooling equipment:

- Vacuum generation system peak power demand: 80 kW
- Vacuum generation system power demand during operations: 50 kW
- Chillers power demand: 13 kW (only chillers for the cooling of the vacuum pumps)
- Cooling power for HVAC: 17.5 kW

## VERT-X Design of Vertical X-Ray Test Facility for ATHENA



Compressed air equipment has the following characteristics:

- Nominal pressure: 6 bar
- Maximum pressure: 7 bar
- Admissible pressure variation: 5-7 bar
- Air pressure required flow rate: 6,6 lt/min for the largest gate valves

Details of power loads for the vacuum generation system are listed in Table 5-2.

## VERT-X Design of Vertical X-Ray Test Facility for ATHENA



LOAD DESCRIPTION	LABEL	SCENARIO					INSTALLED (NOMINAL) POWER				LOAD POWER DEMAND			OTHER INFORMATION				
		Daytime	Night time	Maintenance Mode	UPS	Start up-Shut down	Voltage [V]	Phases	P [kW]	S [kVA]	$P_u = K_u * P$ [kW]	Ppk [kW]	Ku	cosfi	cable diameter (mm)	Location	Cabinet	Note
Pre-vacuum Pump 1	GX450-1	x	x		x	TBD	400Vac or 230 Vac	3	21,10						Attached to vessel		Pre-vacuum: once pre-vacuum is reached, gate valve closes, pump is switched-off	
Pre-vacuum Pump 2	GX450-2	x	x		x	TBD	400Vac or 230 Vac	3	21,10						Attached to vessel		Pre-vacuum: once pre-vacuum is reached, gate valve closes, pump is switched-off	
Pre-vacuum Pump 3	GX450-3	x	x		x	TBD	400Vac or 230 Vac	3	21,10						Attached to vessel		Pre-vacuum Once pre-vacuum is reached, gate valve closes. An electro-valve opens and this pump assists the secondary vacuum circuit to perform pre-vacuum of the turbomolecular pumps volume.	
Mechanical Booster 1	EH2600-1	x	x		x	TBD	400Vac or 230 Vac	3	11,00						Attached to Pre-vacuum Pump 1		Pre-vacuum	

## VERT-X Design of Vertical X-Ray Test Facility for ATHENA



LOAD DESCRIPTION	LABEL	SCENARIO					INSTALLED (NOMINAL) POWER				LOAD POWER DEMAND			OTHER INFORMATION				
		Daytime	Night time	Maintenance Mode	UPS	Start up-Shut down	Voltage [V]	Phases	P [kW]	S [kVA]	$P_u = K_u \cdot P$ [kW]	Ppk [kW]	Ku	cosfi	cable diameter (mm)	Location	Cabinet	Note
Mechanical Booster 2	EH2600-2	x	x		x	TBD	400Vac or 230 Vac	3	11,00							Attached to Pre-vacuum Pump 2		Pre-vacuum
Mechanical Booster 3	EH2600-3	x	x		x	TBD	400Vac or 230 Vac	3	11,00							Attached to Pre-vacuum Pump 3		Pre-vacuum
Pre-vacuum Pump Isolation Valve 1	PV-GV-ISO160-1															Attached to Pre-vacuum Pump 1		ISO DN160, actuated by compressed air
Pre-vacuum Pump Isolation Valve 2	PV-GV-ISO160-2															Attached to Pre-vacuum Pump 2		ISO DN160, actuated by compressed air
Pre-vacuum Pump Isolation Valve 3	PV-GV-ISO160-3															Attached to Pre-vacuum Pump 3		ISO DN160, actuated by compressed air
Medium vacuum Pump 1	STPA4506c-1	x	x		x	TBD	230Vac	3	1,70							Attached to vessel		Secondary vacuum



## VERT-X Design of Vertical X-Ray Test Facility for ATHENA



LOAD DESCRIPTION	LABEL	SCENARIO					INSTALLED (NOMINAL) POWER				LOAD POWER DEMAND			OTHER INFORMATION				
		Daytime	Night time	Maintenance Mode	UPS	Start up-Shut down	Voltage [V]	Phases	P [kW]	S [kVA]	$P_u = K_u \cdot P$ [kW]	Ppk [kW]	Ku	cosfi	cable diameter (mm)	Location	Cabinet	Note
High vacuum Pump 2	COOLVAC5000-2	x	x		x	TBD												Cryo pump
High vacuum Pump Isolation Valve 1																		gate valve (ISO400 o ISO500)
High vacuum Pump Isolation Valve 2																		gate valve (ISO400 o ISO500)
High vacuum Pre-vacuum Dry Pump																		Pre-vacuum pump
Vacuum sensor electrical panel																		Vacuum sensors and panel (5 x Pirani 2 x Penning)

## VERT-X Design of Vertical X-Ray Test Facility for ATHENA



LOAD DESCRIPTION	LABEL	SCENARIO					INSTALLED (NOMINAL) POWER				LOAD POWER DEMAND			OTHER INFORMATION				
		Daytime	Night time	Maintenance Mode	UPS	Start up-Shut down	Voltage [V]	Phases	P [kW]	S [kVA]	$P_u = K_u \cdot P$ [kW]	Ppk [kW]	Ku	cosfi	cable diameter (mm)	Location	Cabinet	Note
Chiller 1																		Cooling units for pre-vacuum
Chiller 2																		Cooling units for cryo and turbo

Table 5-2: VERT-X vacuum generation system main loads power budget

## VERT-X Design of Vertical X-Ray Test Facility for ATHENA



### 5.2. XRS TESTING SYSTEM

Following the preliminary design estimations, mass values of the components of XRS testing system are as reported in Table 5-4.

Part number	Level 1	Level 2	Level 3	Level 4	Level 5	Level 6	Level 7	Level 8	Mass [kg]
<b>30-00-00-00-00</b>	<b>XRS testing system</b>								<b>8340</b>
<b>31-00-00-00-00</b>		<b>raster scan</b>							<b>7780</b>
31-10-00-00-00			base						<b>5800</b>
31-11-00-00-00				welded assembly					5600
31-20-00-00-00			translation X frame						<b>1170</b>
31-21-00-00-00				welded assembly					790
31-30-00-00-00			translation Y frame						<b>260</b>
31-31-00-00-00				welded assembly					210
31-40-00-00-00			rotation X frame						<b>250</b>
31-41-00-00-00				welded assembly					160
31-50-00-00-00			X-ray tube assembly						<b>300</b>
31-51-00-00-00				X-ray source					40
31-51-10-00-00					interface				39
31-52-00-00-00			collimator system						90
31-52-10-00-00					interface				10
31-53-00-00-00			monochromator						
31-53-10-00-00					interface				5
31-54-00-00-00			axis welded assembly						60
31-55-00-00-00			carbon fibre tube						35
<b>32-00-00-00-00</b>		<b>MA</b>							<b>400</b>
32-10-00-00-00			MGSE						
32-20-00-00-00			gravity release system						400
32-30-00-00-00			MA						
<b>33-00-00-00-00</b>		<b>detection</b>							<b>TBD</b>
33-10-00-00-00			MGSE						
33-20-00-00-00			positioner						
33-30-00-00-00			detector						
<b>34-00-00-00-00</b>		<b>metrology</b>							<b>160</b>
34-10-00-00-00			tip-tilt metrology						<b>0</b>
34-11-00-00-00			optical T-T metrology						
34-11-10-00-00			rotation X detection system						
34-11-11-00-00					external station				
34-11-12-00-00					vacuum optical train				
34-11-13-00-00					reference mirror				
34-11-20-00-00			rotation Y detection system						
34-11-21-00-00					external station				
34-11-22-00-00					vacuum optical train				
34-11-23-00-00					reference mirror				
34-12-00-00-00			tiltmeters						
34-20-00-00-00			linear displacement metrology						160

## VERT-X Design of Vertical X-Ray Test Facility for ATHENA



Part number	Level 1	Level 2	Level 3	Level 4	Level 5	Level 6	Level 7	Level 8	Mass [kg]	
34-21-00-00-00				internal displacement metrology						160
34-21-10-00-00					external station				100	
34-21-20-00-00					vessel floor station				45	
34-21-30-00-00					RS station				5	
34-21-40-00-00					MA station				5	
34-21-50-00-00					detector station				5	
34-22-00-00-00				external displacement metrology						
34-22-10-00-00					external station					
34-22-11-00-00					mechanical support					
34-22-12-00-00					laser tracker					
34-22-20-00-00					retro-reflectors					

Table 5-3: VERT-X XRS testing system mass budget

### 5.3. X-RAY SOURCE AND COLLIMATOR

The available technical parameters of the X-ray source are listed in Table 5-4. The details in the table are referred to the Sigray X-ray source that is the current baseline for VERT-X design.

Parameter	X-ray source	Source chiller	Ion pump controller
Dimensions	35 cm x 8 cm x 14 cm	33 cm x 28 cm x 33 cm	14 cm x 9 cm x 25 cm
Voltage	115 V, 60 Hz	115 V, 60 Hz	115 V, 60 Hz
Power supply	100 W	500 W (TBC)	100 W (TBC)

Table 5-4: X-ray source technical parameters

According to the current VERT-X design, the technical budget for the collimator optics is as listed in Table 5-5.

Parameter	Collimator
Mirror size	12 cm x 12 cm x 114 cm
Mirror weight	40 kg
Mirror holders weight	10 kg

Table 5-5: Collimator mirror technical parameters

## VERT-X Design of Vertical X-Ray Test Facility for ATHENA



### 5.4. DETECTION ASSEMBLY

For the detection assembly the technical parameters of the Sydor camera and the Axis Photonique camera are listed in Table 5-6. The former is the option proposed at the beginning of the study as baseline for VERT-X camera system, the latter represents an alternate, more affordable solution based on a new detector developed by GPIXEL company and a design by Synchrotron Soleil.

Indeed, the sensor used in the Axis Photonique camera has a limited efficiency because of its thinness. Nevertheless, this problem is expected to be superseded thanks to the Einstein Probe Team that plan to use the GPIXEL detector for their experiment and are promoting the development of an improved version of it, with a thicker and larger configuration and hence a better working efficiency. Accordingly, a full camera based on the enhanced GPIXEL detector is under development. For this reason, a third option may be expected to be added in the future to the two options of Table 5-6.

Parameter	Sydor camera	Axis Photonique camera
Weight	4 kg	4 kg
Size	9 cm x 11 cm x 12 cm	12 cm x 12 cm x 14 cm
Voltage	230 VAC / 60 Hz	TBD VAC
Power supply	300 W	TBD

*Table 5-6: Available technical budget details for Sigray and Axis Photonique cameras*

For the detector (x, y, z) positioning stage, the proposed baseline includes a hexapod for the fine movement along x, y and z and two brushless engines for the translation of the camera and hexapod assembly to the position for the X-ray source calibration.

Voltage supply is 12 V + 24 V for the hexapod while for the two engines the voltage supply is from 220 V to 380÷400 VAC 3P. More specific values of voltage supply, as well as power supply demand, will be available with the final selection of the engines.